Chapter 4

Investigating the Nature of Insulator-Metal Transition in Neutron-Transmutation-Doped Ge:Ga

Samy Abd-elhakim Elsayed

Additional information is available at the end of the chapter

http://dx.doi.org/10.5772/intechopen.72241

Abstract

n-type germanium samples irradiated with fast reactor neutrons with a fluency range from 2×10^{16} up to 1×10^{20} cm^{-2}. As a result of irradiation, n-Ge samples are converted into p-type Ge. The dc conductivity is measured in wide temperature range from 1.5 up to 300 K. Insulator metal transition occurs at irradiation fluency 5×10^{18} cm^{-2}. The Bohr's radius of localization (a_H) is obtained and found to be equal to 43 Å. Mott variable range hopping and Shklovskii-Efros percolation models are applicable in the present data.

Keywords: germanium, irradiation disordered, insulator-metal transition, Mott variable range hopping, percolation theory of conduction, Anderson transition

1. Introduction

1.1. Ionizing and non-ionizing radiations

Sun light consists of electromagnetic (EM) waves, which provide light and heat. Sunlight electromagnetic waves consist of infrared (IR), visible, and ultraviolet (UV) frequencies; as the color goes more into blue, the wavelength decreases and the frequency increases and vice versa, as the color goes into red color, the wave length increases and frequency decreases. Generally, the EM radiations are divided into two categories depending on wavelength ionizing and non-ionizing. This division depends on the radiation energy or frequency; high frequency radiation ($>3 \times 10^{15}$ Hz) is ionizing radiation and low frequency radiation ($<3 \times 10^{15}$ Hz) is nonionizing radiation [1]. When a substance absorbs the EM radiation with a frequency lower than 3×10^{15} Hz, excitation occurs, and the radiation excites the motion of molecules, or excites an electron from occupied orbital into an empty higher energy orbital. But if the absorbed EM radiation has frequency greater than

3×10^{15} Hz, ionization occurs, that is, removing an electron from an atom or molecule. The atom consists of nucleus and extranuclear structure. The extranuclear structure consists of electrons revolving around the nucleus in certain energy levels; each level contains a restricted number of electrons when an electron jumps from high energy level down to lower energy level; an EM radiation with energy equal to the difference between the two energy levels emits from the atom. When an electron jumps from high energy level to the low energy level, a high frequency $\cong 3 \times 10^{17}$ Hz emits from the atom, this is X-ray radiation. The X-ray radiation is an ionizing radiation. The nucleus consists of protons which have positive charge equal to the electron charge and mass 1.67×10^{-27} Kg. The number of protons in the nucleus equals the number of electrons outside the nucleus and the number of protons or electrons of an atom is denoted by Z (the atomic number) and neutrons which have no electric charge, but have magnetic moment. The number of neutrons is denoted by N. The total number of protons plus neutrons in a nucleus is denoted by A = Z + N (the mass number) [2]. When the nucleus is stable, no irradiation emits from it, but some heavy nuclei excited "not stable" and need to emit some energy to reduce their energies and become more stable [3]. The nucleus emits very high EM radiations, which are gamma rays. Gamma rays have frequency 3×10^{20} Hz, and are ionizing radiations. The unstable nuclei may also emit β particles, protons or neutrons, and/or α-particles, which is the nucleus of He^{++} atom; sometimes, the nucleus emits high energy electromagnetic radiation gamma waves (γ). The stable nucleus is characterized by the mass number A, and the atomic number of protons' number (Z) which equals the number of neutrons (N). In large nuclei $N \cong 1.7\ Z$, repulsion between protons causes instability in the nucleus. This instability decreases if the number of neutrons excesses the number of protons. Instable nucleus, such as U^{238}, emits radiation. This is called natural radioactivity. Nuclear radioactivity involves three kinds of radiations: α, β, and γ radiations. Each of these radiations has distinct properties. Examples of artificial radioactivity are: when α particle collide with aluminum a proton is rejected leaving a stable silicon isotope $Al_{13}^{27} + He_2^4 \rightarrow Si_{14}^{30} + H_1^1$ or a neutron rejected leaving an isotope of phosphorus $Al_{13}^{27} + He_2^4 \rightarrow P_{15}^{30} + n_0^1$ and this phosphorus element is instable and disintegrates into silicon by emission of positron $P_{15}^{30} \rightarrow S_{14}^{30} + e^+$. This type of nuclear reaction has technological application [4], opens the way of peaceful using of nuclear power, in doping semiconductor by nuclear irradiation. Semiconductor industry is playing a very important role for mankind's everyday life and economic growth. The most famous radioactive semiconductor materials' doping is the neutron transmutation doping (NTD). This new technology is used in doping semiconductor materials such as germanium and silicon; the advantages of this new method are (i) homogenous distribution of doping atoms in the host material, (ii) controlling the concentration of doping atoms by controlling the irradiation dose, and (iii) controlling the compensation K in the host material. This new technology opens the way into tailoring materials with definite conductivity at definite temperature for a certain technology application. For example:

$$
\begin{aligned}
&{}^{74}Ge(n,\gamma)^{75}Ge \xrightarrow[82\text{min}]{\beta} {}^{75}As + \nu \\
&{}^{76}Ge(n,\gamma)^{77}Ge \xrightarrow[11.3hr]{\beta} {}^{77}As + \nu \\
&{}^{77}As \xrightarrow[38.3hr]{\beta} {}^{77}Se + \nu \\
&{}^{70}Ge(n,\gamma)^{71}Ge \xrightarrow[11.4day]{\varepsilon} {}^{71}Ga + \nu
\end{aligned}
\tag{1}
$$

But (NTD) has disadvantages like: (i) irradiation cost, (ii) reduction in minority carrier life time, and (iii) radioactive safeguards considerations.

n-germanium irradiated reactor neutrons and/or γ converted into p-type germanium [5].

2. Effect of ionizing radiation on the electrical properties of semiconductors

The electrical conductivity of solids ranges from $10^{9}(\Omega.cm)^{-1}$ for pure metal such as copper at liquid helium temperature to at most 10^{-22} $(\Omega.cm)^{-1}$ for the best insulators or nonmetals at the same temperature [6]. These vast differences in electrical conductivity separates the metallic and non-metallic states of matter, this variation amounts to a factor at least 10^{31}, which is probably widest variation for any physical property. Therefore, from electrical conduction characteristics, it is well-known that solid materials are divided into four categories:

i. Metallic conduction (good electrical conductors with electrical conductivity that reaches to $10^{9}(\Omega.cm)^{-1}$ at liquid helium temperature)

ii. Insulators (Poor electrical conduction with electrical conductivity that reaches to $10^{-22}(\Omega.cm)^{-1}$ at liquid helium temperature)

iii. Semiconductors, this type of materials distinguishes from metals and insulators by their negative coefficient of resistance (their resistance decreases with increasing temperature, while in metals it increases)

iv. Super-conductors, in this class of materials, the resistance vanishes at low temperatures, the temperature at which resistance vanishes depends on the material's type, composition, structure, and preparation method.

This chapter focused on the transition between metallic and insulator phases of conduction. Mott is first one who recognized the problem of metal-insulator transition [7]. He noticed that, although the band theory successfully explained the electronic structure of solids, it explains why some materials have metallic conductivity, other semiconductors, or insulators. But, the band theory gives incorrect ground states of some transition metal oxides such as CoO, MnO, and NiO. In the case of CoO, for example, CoO has NaCl-like structure with a unit cell containing one Co atom and one O atom. The outer shell of the Co atom has an electron configuration of 3d4s, and the O atom 2S2P, that means, the number of electrons per unit cell is 9 + 6 = 15, an odd number. Band theory predicted that crystals with unit cell containing an odd number of electrons should have metallic conductivity behavior. But experimentally it is proved that CoO is actually an insulator with a large gap. These transition metal oxides are called Mott insulators [8] and were first inadequate of band theory. Mott said there is something wrong in band theory. What is that? Mott discussed the band theory in that although it had succeeded in explaining the cause of some materials having metallic conductivity, other semiconductors, and insulators, the band theory neglected the correlation between electrons. These transition metal oxides contain strongly correlated electrons, so the band theory fails in such systems with strongly correlated electrons. Mott started from the model suggested by

Bloch which is called "collective electron model." In this model, the electrons in the outermost shell of the atoms concerned are not supposed to be bound to their individual atoms, but are assumed to be free to move through the lattice under the effect of the atomic cores and the average field of the other electrons. This field is periodic with the period of the lattice. Mott criticized this model that the electrons tend to keep away from one another because of the Coulomb's repulsive force. In metals, each electron carries with it a surrounding sphere, into which other electrons are unlikely to come. In insulators, one of the electrons in outermost shell of an electron will not be able to move to the next atom unless an electron from the next atom gets out to create a free place to it. Mott declares that the collective electron model cannot explain the optical absorption in insulators [8].

For many years Mott insulators were neglected by most authors of solid state physics text books. By the discovery of high T_C superconductors in cuprates and the rediscovery of colossal magnetoresistance in manganite's the situation changed. These materials have proved to be doped-Mott insulators. So, the physics of Mott insulators and doped Mott insulators become important in contemporary research in condensed matter physics. The main problem for Mott insulators is to find the correlation energy of the electrons. It is Hubbard energy U for double occupancy of the same orbital on the same atomic site by two electrons. Mott starts to solve the problem of strongly correlated electrons. He supposed that for an array of electrons centers with cubic structure, there are two possibilities. The first is that the crystal is metal and the second is an antiferromagnetic insulator. But an antiferromagnetic lattice can split the conduction band into full and empty bands, these are called Hubbard bands, the insulating behavior does not depend on antiferromagnetic order, and continues above Neel temperature [9].

3. Mott metal-insulator transition (MIT)

3.1. Transition metals and their alloys

Transition metals are the metals with incomplete d state in atomic structures like Co, Fe, Ni, Cd, etc. In magnetic transition metal compounds, the conduction electrons lie wholly in a d-band, with some extent of hybridization with 4s electrons. This means that the d- band is separated from conduction band and contains an integer number of electrons per atom. And a band containing an integer number of electrons must exceed a certain width if it is to be metallic. Based on Gutzweller [10], approximation of variational calculation method of the ground state wave-function for model Hamiltonian with single-binding band and with only intra-atomic Coulomb interaction between the electrons, considering the case in which one electron per atom and, they found that the Gutzweller variational state is always metallic [11]. The experimental results of Craig et al. [12] on the electrical resistivity of Ni near its Curie temperature lead Fisher et al. [13] to criticize the theoretical treatment of resistive anomaly theory suggested by de Gennes and Frieddel [14] because, in their treatment they supposed long-range fluctuations of the magnetization near the critical point and this lead to incorrect result, but the short-range order fluctuations which make the dominant contribution to the temperature dependence of resistivity. Monecke et al. [15] investigated the specific heat of the

http://dx.doi.org/10.5772/intechopen.72241

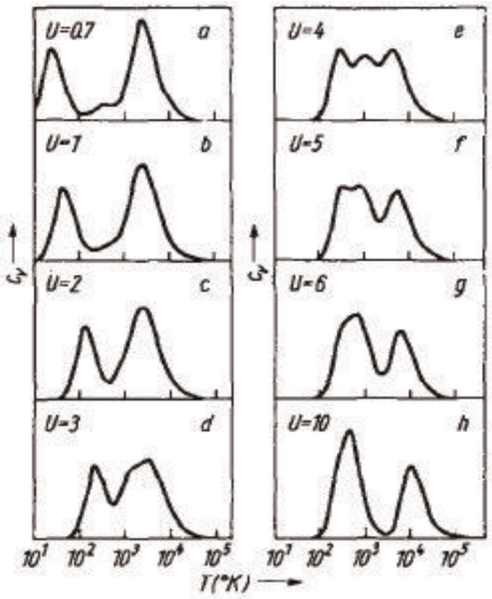

Figure 1. C_v dependence on temperature at different values of Hubbard energy.

Hubbard system which consists of four atoms and four electrons, in wide temperature range from 10 K up to 10^5 K. And, he found that in the specific heat C_v dependence on temperature, as seen in **Figure 1**, there are three maxima, two of them related to Néel transition and sudden change in magnitude of magnetic moment and the third maxima proved as Mott transition [7].

3.2. Mott metal insulator transition

Mott started to explain the metal insulator transition on the basis of Hubbard band model [16]. Mott outlines the properties of a crystalline array of one-electron centers, each described by a wavefunction φ(r) behaving as exp.(−r/a_H) for large r, at distance a from each other, sufficiently large for the tight binding approximation to be useful. If the number of electron per atom deviates from integral value, the model should always predict metallic behavior, but with one or any integral number of electrons per atom this is not so, and the system is insulating [7]. The most convenient description is in terms of Hubbard intra-atomic energy U which is defined by

$$U = \iint \left(\frac{e^2}{kr_{12}}\left|\phi(r_{12}\right|^2\left|\phi(r_2\right|^2 d^3x_1 d^3x_2 \tag{2}$$

For hydrogen-like atom

$$U = \frac{5e^2}{8ka_H}$$

If P is the ionization potential of each atom and E is the electron affinity, by assuming that the functions φ are not changed by addition of an extra electron

$$U = P–E \tag{3}$$

The properties of such system are the following:

i. when the distance a between the centers is large, the overlap energy integral ***I*** is small, the system is expected to be antiferromagnetic, with energy below that of the ferromagnetic state equal to $-2zI^2/U = -B/(2zU)$, where B is the band width $B = 2zI$. The Néel temperature T_N will be such that kT_N is of this order.

ii. An extra electron placed on one of the atoms is able to move with a k vector just as in normal band. It proposed to have an energy in the "upper Hubbard band." It well polarizes the spins on surrounding atoms antiparallel to itself, or parallel if the atomic orbitals are degenerate, forming a "spin polaron." Its bandwidth is probably not very different from B calculated without correction.

iii. A hole formed by taking an electron away from one atom has similar properties, being able to move with wavevector k and having a range of energies not very different from B.

iv. The two bands will overlap when a is small enough, and consequently B great enough, to ensure that

$$B \geq U$$

A metal-insulator transition then occurs, sometimes known as "Mott transition."

The Mott transition is similar to the band crossing transition, being from antiferromagnetic insulator to antiferromagnetic metal. As the overlap increases, the number n of free carriers increases, the moment on the atoms and Neel temperature will tend to zero and disappear when $n = 1/2z$. **Figure 2** shows magnetic moment and Néel temperature at the transition between antiferromagnetism and normal metal against B/U [7], here we have two situations; first, the antiferromagnetism is absent, and after the magnetic moment have disappeared the electron gas becomes highly correlated, this means that small proportion ζ of the sites are doubly occupied at any moment, or unoccupied and the spins of the electrons on other sites

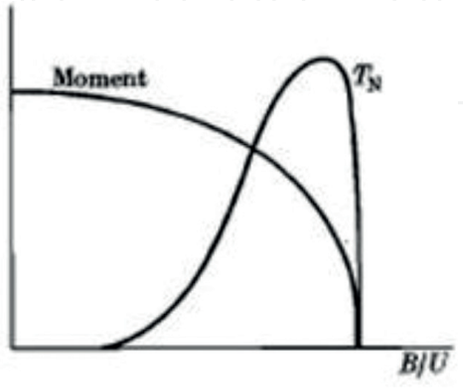

Figure 2. Magnetic moment and Nèel temperature at transition antiferromagnetism and normal metal as function of B/U.

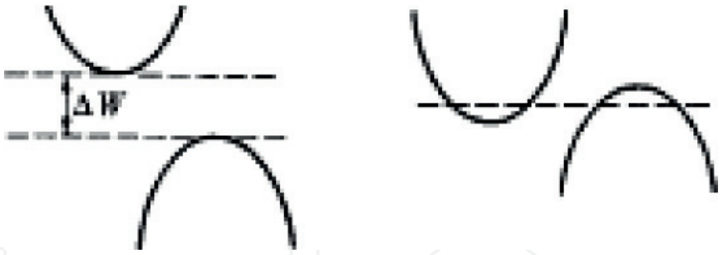

Figure 3. Two Hubbard bands overlapped in metal case, and not overlapped in insulator non-metal.

are no longer arranged antiferromagnetically, but resonate quantum mechanically between their two positions. The band is no longer split into two Hubbard bands **Figure 3**; instead there is a large enhancement by 1/2ζ of the effective mass. The simplest form of metal-insulator transition is the form of semi-metal, a material for which the conduction and valence band overlap, to a non-metal, where there is no overlap.

In the antiferromagnetic insulator, the magnitude of the Hubbard gap is not greatly affected when the temperature goes through the Neel point T_N. The Hubbard gap is then, essentially, the energy required to take an electron from an atom and put it on a distant atom where another electron is already present. The energy U needed to achieve this does not depend on coexistence of the antiferromagnetic long-range order. At zero temperature, an insulator can be described in terms of the full and empty bands determined by long-range antiferromagnetic order. In simple cubic lattice of one electron centers, if U/B > 0.27, a sharp metal-insulator transition occurs above Néel temperature. But it has been found that above Néel temperature, for a rigid lattice, the transition between an antiferromagnetic insulator and a metal as U/B varies is not sharp; Mott thought that this is a result of considering the long-range forces in Hubbard model [16]. As the temperature increases [17], the electrons are excited into the conduction band, their coupling with moments lowers the Néel temperature. Thus, the disordering of the spins with consequent increase of entropy is accelerated. Ramirez et al. [18] showed that a first-order transition to degenerate gas in the conduction band, together with disordering of the moments, is possible.

At the transition, the value of B ≥U can be evaluated for hydrogen like wavefunction, $U = \frac{e^2}{8ka_H}$ since both U and B are known

$$I = I_o e^{-\alpha R}$$
$$I_o = \left\{\frac{3}{2}(1+\alpha R) + \frac{1}{6}(\alpha R)^2\right\} e^2\alpha \tag{4}$$

I is the overlap energy integral

$$\alpha = \frac{(2mW_0)^{1/2}}{\hbar}$$

and α is defined as the distance at which the single-well wavefunction exp.$(-\alpha R)$ falls off. Since the value of B near the transition is given by

$$B = 23z\left(\frac{e^2\alpha}{k}\right)e^{-\alpha R} \tag{5}$$

but because of the rapid variation of $e^{-\alpha R}$ and αR depend on z; αR = 5.8 [28], and if z the coordination number = 6

$$n^{1/3}a_H \cong 0.2 \tag{6}$$

This equation is used for the discussion of metal insulator transition in doped semiconductors.

3.3. Anderson insulator metal transition

Anderson [19] showed that at a certain randomness, the electron wavefunction becomes localized. According to the Anderson model, as shown in **Figure 4**, there exists a critical value V_O/B above which the diffusion is impossible at zero temperature. Anderson introduced a random potential into each well within limits $\pm\frac{1}{2}V_o$. This leads to finite mean free path l such that $a/l = 0.7(V_O/B)^2$. If $V_O/B \cong 1$, the value of l approaches unity. Mott and Kavah [17] showed that it cannot be smaller, and the wavefunction has the form

$$\Psi_{ext} = \sum_n C_n \exp(i\varphi_n)\psi_n \tag{7}$$

where C_n are coefficients, φ_n are random phases, as the V_O/B increases greater than unity the phases still random, the scatter of the coefficients C_n will increase, and the wave function becomes localized having the form

$$\Psi = Rral[\psi_{ext}]\left\{e^{\frac{-(r+r_O)}{\zeta}}\right\} \tag{8}$$

where r_o is some point in space, and ζ is the localization length. The critical value of V_o/B depends on the co-ordination number z. Mott and Kavah [17] supposed that V_o/B greater than unity, the range of energies in the band increased to $(v_o^2 + B^2)^{0.5}$, so they write in the mid-gab

$$N(E) = 1/\left\{a^3\left(v_o^2 + B^2\right)^{0.5}\right\} \tag{9}$$

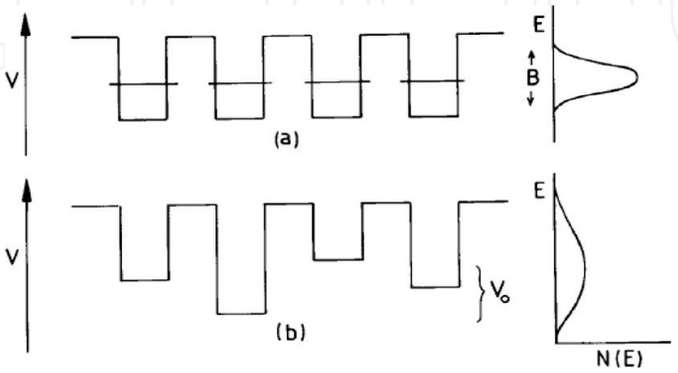

Figure 4. The potential energy of an electron in the Anderson model: (a) without a random potential, and (b) with a random potential V_O. B is the band-width in case (a). The density of states N(E) is shown.

http://dx.doi.org/10.5772/intechopen.72241

3.4. Mott versus Anderson explanation of metal-insulator transition

Mott treated the metal-insulator transition problem by considering the electron gas as screening the positive charge on the donors, so the potential energy seen by electrons in heavily doped semiconductors is of the form

$$V(r) = \frac{e^2}{kr} e^{-qr} \tag{10}$$

where k is the dielectric constant of the semiconductors, and q is the screening constant depending on the electron density n. Mott also proposed that for an electron which its potential energy follows formula $v(r) = (e^2/kr) \exp.(-qr)$ and if q is large enough the electron gas would have metallic properties. But as the density of electron gas drops, bound states become possible. By calculation, the value of n at which the transition occurs to be

$$n^{\frac{1}{3}} a_H = 0.25 \tag{11}$$

where a_H is the Bohr radius of donors. It is predicted that a discontinuous transition would occur from a state at which all electrons were bound to donors to one in which they were free, this is Mott transition. Mott [7] predicted that at the transition, the indirect band gap should disappear. This proved in germanium and silicon. In these semiconductor materials, in case of electrons and holes production by irradiation, electrons and holes combine at low temperature to form excitons, which are for indirect band gap have comparatively long-life time. Excitons attract each other and droplets of an electron-hole gas formed. The electron-hole gas droplets have two forms; one is the excitonic insulator, or an electron-hole metallic gas. Mott and Kavah [17] argued that if V_o/B is less than critical value, the states are localized up to mobility edge. As shown in **Figures 4** and **5**, the localization length ξ tends to infinity as $E \rightarrow E_c$, if we write $a/\xi = \text{const.}\ (E_c - E)^s$, neither the constant nor the index is known with certainly.

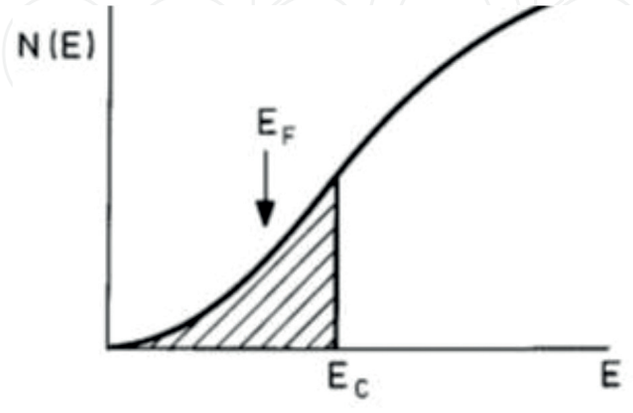

Figure 5. Density of states with potential energy of **Figure 4** showing the mobility edge E_c. The position of the Fermi energy E_F below E_C is shown.

3.5. Conductivity of a metal in Anderson model

The conductivity of a metal is due to a gas non-interacting electron in the field of Anderson random potential. The conductivity of a metal is usually written in the form $\sigma = ne^2\tau/m$, where n is the number of electrons per unit volume, m is the effective mass, and τ is the time of relaxation. If l is the mean free path, S_F is the Fermi surface area $4\pi k_F$, and $n = (8\pi/3)k_F^3/8\pi^3$, σ takes the form $\sigma = S_F e^2 \iota/12\pi^3\hbar$, Mott and Kavah [17] examined the last formula mean free path l = a, at z = 6 n = $1/a^3$, hence $K_F a = K_F l = (3\pi^2)^{1/3} \cong 3.1$, the conductivity is thus:

$$\sigma \cong \frac{1}{3}\left(\frac{e^2}{\hbar a}\right) \tag{12}$$

This last equation assumes a spherical Fermi surface; if a = 2 Å, the numerical value is 3000 $(\Omega.cm)^{-1}$. But Mott and Kavah expected the smallest conductivity in the range 2–5000 $(\Omega.cm)^{-1}$.

As the ratio V_o/B increases the conductivity decreases because

i. As the density of states at E_F decreases, the conductivity decreases, and may be written in the form $\sigma = \frac{1}{3}\left(\frac{e^2}{\hbar a}\right)g^2$,

ii. Where,

$$g = \frac{B}{\left\{1.75\left(B^2 - V_o^2\right)^{\frac{1}{2}}\right\}}$$

In this case a minimum metallic conductivity expected, and given by

$$\sigma_{\min} = \frac{e^2}{3\hbar a} g_c^2 \approx 0.03\frac{e^2}{\hbar a,}, \quad g_c \cong 1/3 \tag{13}$$

g_c is the critical value at Anderson localization

iii. As the ratio V_o/B increases, another phenomenon appears which is called incipient localization, this phenomenon decreases the conductivity, $\sigma \to 0$ as T tends continuously to zero, as V_o/B increases to the critical value.

The Anderson transition is a phenomenon in which some systems for example, doped semiconductors, the zero temperature Fermi energy move from point above the mobility edge to a point below it. Generally, σ goes continuously to zero, as shown in **Figure 6a**, but if the transition is induced by magnetic field H, very sharp transition occurs as shown in **Figure 6b**. The conductivity at zero-field mobility edge E_c (0) is given by

$$\begin{aligned} &\sigma(E_C(0)) = 0.03\frac{e^2}{\hbar L}, L = L_H = \left(\frac{c\hbar}{eH}\right)^{\frac{1}{2}} L > a \\ &L = a \ldots\ldots\ldots\ldots\ldots\ldots\ldots\ldots\ldots L_H < a \end{aligned} \tag{14}$$

As a conclusion of this section, in Mott model, the metal insulator transition occurs because the correlated electron gas cause increasing in the distance between the atomic centers in the lattice. There is a minimum metallic conductivity given by

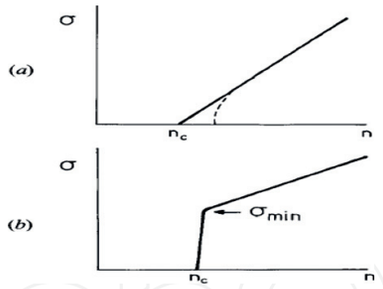

Figure 6. The behavior of conductivity at zero temperature of a degenerate electron gas as a function of charge carrier concentration n, so the E_F moves through the mobility edge E_C, (a) if σ_{min} does not exist and (b) if it does. The broken line shows the possible effects of interactions.

$$\sigma_{\min} = \frac{0.03e^2}{\hbar L_i}$$

where L_i is the inelastic diffusion length, and the transition is a first-order transition. Meanwhile, Anderson transition metal insulator occurs because the existence of disorder, as the disorder increasing the wave function becomes nonlocalized (metallic state) and the transition is continuously occurring, and becomes sharp only under the effect of external magnetic field, and there is no minimum metallic conductivity.

4. Experimental part

Samples of germanium doped with Arsenic irradiated with fast neutrons with energies of $E \geq 0.1$ MeV in the range of $2 \times 10^{16} \leq \Phi \leq 1 \times 10^{20}$ cm^{-2}. As a result of irradiation, all the original samples become disordered p-type [20–23]. In order to reduce the transmutation doping effect, all samples were placed in 1-mm-thick cadmium containers. During irradiation in the reactor, the ratio between thermal neutrons fluency and the fluency of fast neutrons was about 10. So, it was possible to obtain samples of germanium "doped" with acceptor-like radiation defects {Ge (RD)}. To ensure that the electrical properties were controlled by the transmutation doping, a complete annealing at 450°C for 24 h was performed. For electrical resistivity measurements, a special double wall glassy cryostat is designed [24]. This cryostat is attached with vacuum pump its evacuation rate is faster than the evaporation rate of He^4 gas, thus the pressure inside the cryostat is decreased and hence the temperature. The conventional four probe method is used for electrical resistivity measurements. Ni electrode is participated in the desired position on the samples using electrochemical deposition technique (cold method). Thin Cu wires are fixed above the Ni electrodes using In. The samples were in parallelepiped shape with length about 8–12 mm, thickness about 1–2 mm, width about 2–3 mm, and the electrode apart about 3–4 mm resistivity of Ge (RD) was measured in the temperature range from 1.7 up to 300 K. The temperature was determined with a semiconductor thermistor in the interval 77.4–4.2 K, from saturated vapor pressure of He^4 in the interval 4.2–1.5 K. The voltage across samples always less than 1 V and the current across the sample

decreases from μA to nA order as the temperature lowered. The electrical properties of Ge (RD) are determined solely by acceptor-like radiation defects [25, 26]. The least square fitting method, using a computer program Excel 2010, is used to analysis the data extracted and to calculate the uncertainty in the obtained results.

5. Experimental results

Figure 7 shows the resistivity dependence on temperature of germanium samples irradiated with different doses of neutron irradiation. From this figure, the conductivity activation energy of conductivity ($\sigma = \rho^{-1}$) is obtained, from the empirical equation argued by Fritzche [27]

$$\rho = \rho_o \exp. - (E_C - E_F)/KT + \rho_1 \exp. - (E_A - E_F + W_1)/KT + \rho_2 \exp.(W)/KT \qquad (15)$$

where the term (ρ_o exp.-(E_C-E_F)/KT) represents transport by carriers excited beyond the mobility edge into non-localized (extended) states at E_C or E_V. And ρ is the resistivity, ρ_o is the pre-exponential factor. A plot of lnρ versus 1/T will yield a straight line if E_C-E_F is a linear function of T over the temperature range measured. As the temperature decreases, transport carriers excited into localized states at the band edges and the resistivity is given by ρ_1 exp.-(E_A-E_F + W_1)/KT, where W_1 is the activation energy for carriers hopping, W_1 should decrease with decreasing temperature [28] On the account of variable-range nature of the hopping transport. However, as the temperature dependence is through the carrier activation term, approximately linear dependence of ln ρ versus 1/T is again expected. As the temperature lowered more, there

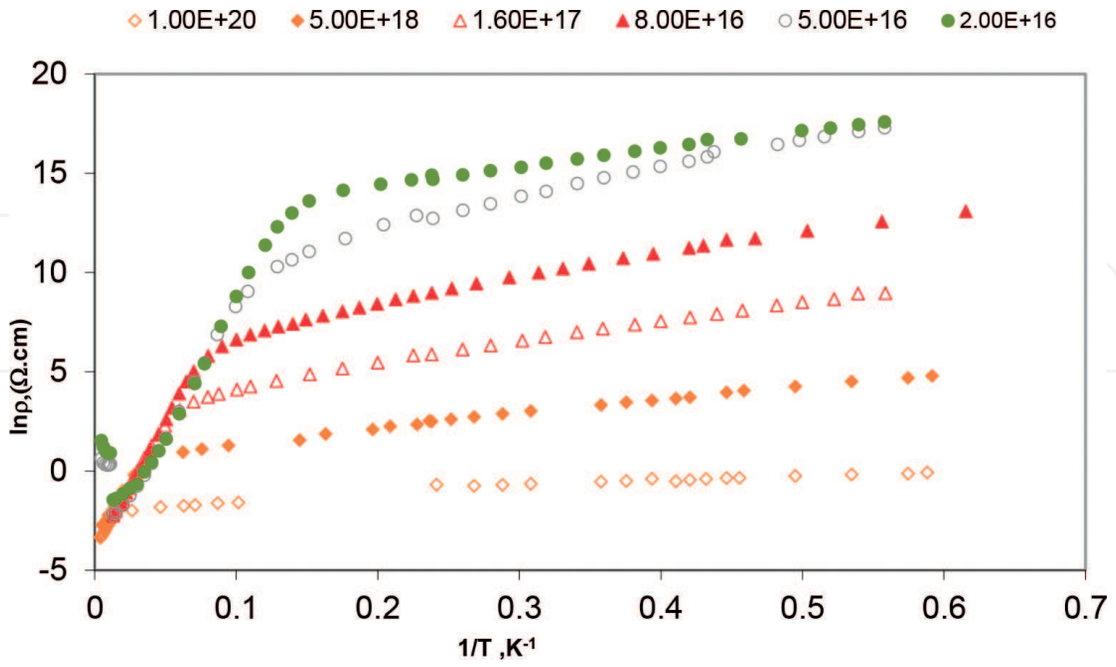

Figure 7. ln σ = f (1/T).

will be a contribution from carriers with energies near E_F which can hop between localized states. This contribution is described by ρ_2 exp. (-W)/KT, where $\rho_1 \leq \rho_2$ and W is the hopping energy of the order of half the width of the band of the states. The extracted results from **Figure 7** are summarized in **Table 1**.

F is the neutron flux, P_{300}, P_{77} are the number of charge carriers at 300 K and 77 K respectively where E_1, E_2, E_3, are the activation energies of different conductivity mechanisms. And m_{300}, m_{77}, are the mobility of charge carriers at 300 K and, 77 K respectively.

The obtained results reveal that $E_1 > E_2 > E_3$, and $\rho_o < \rho_1 < \rho_2$ for all samples.

Figure 8 shows the dependence of resistivity on square root of temperature. This figure is required to apply Shklovskii's percolation theory of conduction where [29]

$$\rho = \rho_o e^{\left(\frac{T_{ES}}{T}\right)^{05}} \tag{16}$$

From this equation, T_{ES} is obtained for each irradiation dose

$$T_{ES} = \frac{\beta e^2}{ka}$$

where β is a constant, e is the electronic charge, k is the dielectric constant, and a is the localization radius.

Figure 9 shows the dependence of resistivity on $T^{-0.25}$. From this figure [30], Mott variable range hopping is applied to obtain Mott characteristic temperature from the equation

Φ, cm^{-2}	**p300**	**logp300**	**p77**	**E_1, meV**	**E_2, meV**	**E_3, meV**	**Logμ_{300}**	**Logμ_{77}**
0	1.6E + 15	15.20	1.5E + 15	21.2	————	————	3.59	4.32
1E + 15	1.5E + 15	15.18	3.3E + 14	28.9	————	————	3.42	4.24
5E + 15	2.5E + 15	15.4	9E + 14	22.6	————	2.27	3.45	4.24
2E + 16	5E + 15	15.7	2.23E + 15	17.8	0.73	0.79	3.39	4.17
5E + 16	1.15E + 16	16.06	6.56E + 15	11.5	1.93	0.84	3.4	3.87
8E + 16	3.7E + 16	16.57	1.18E + 16	10.7	1.57	0.92	3.45	3.64
1.6E + 17	7.4E + 16	16.87	2.2E + 16	9.2	0	0.9	3.45	3.53
5E + 18	1.4E + 17	17.14	4.05E + 16	6.4	————	0.63	3.48	3.23
1E + 20	4.18E + 17	17.62	1.6E + 17	3.7	0	0.03	2.99	2.69

Table 1. The concentration of holes at 300 K and at 77 K, the conductivity activation energies of the three stages of conductivity, E_1 which is the band to band transition activation energy, E_2 which is activation energy of inter band transition activation energy, E_3 which is the hopping conduction activation energy, the mobility μ of holes at 300 K and 77 K, respectively.

$$\rho = \rho_o e^{\left(\frac{T_M}{T}\right)^{0.25}} \tag{17}$$

where $T_M = \frac{\beta_o}{N(E_F)a^3}$, where β_o is a constant, $N(E_F)$ is the density of states at Fermi level, and a is Bohr radius of localization.

The obtained values of T_M and T_{ES} from **Figures 8** and **9** are given in **Table 2**.

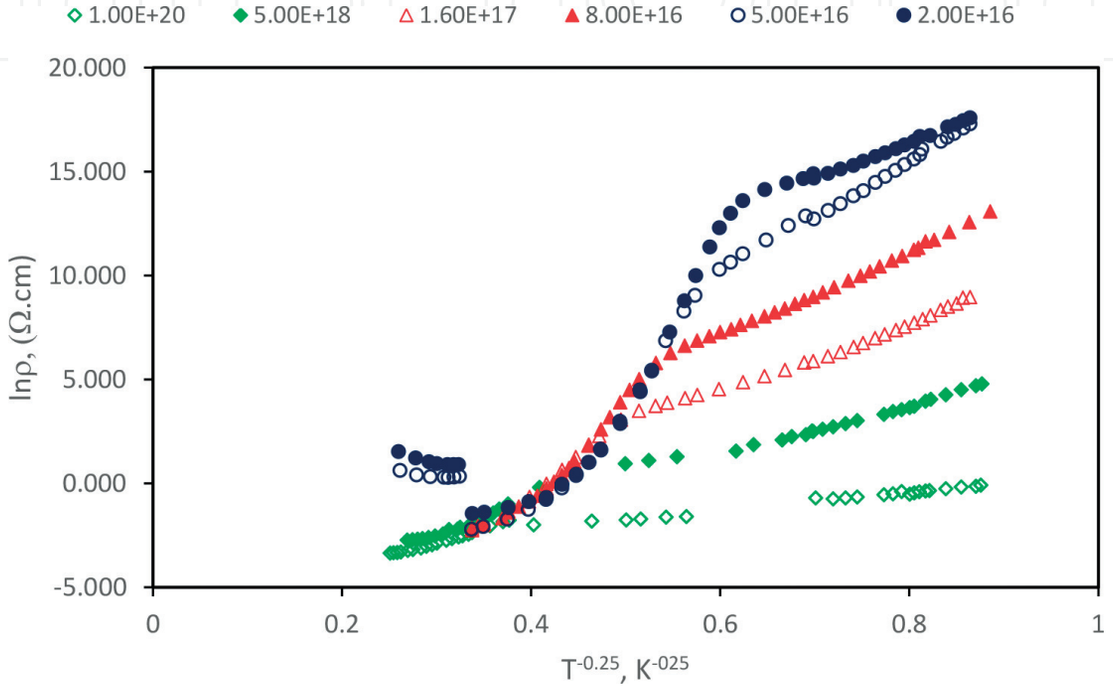

Figure 8. $\ln \sigma = f\,(1/T^{0.5})$.

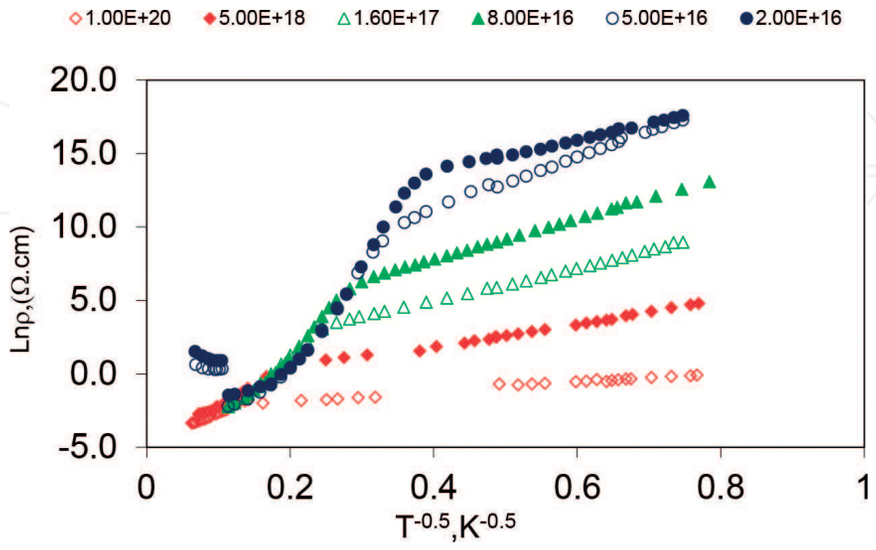

Figure 9. $\ln(\sigma) = f(1/T^{0.25})$.

Φ, cm^{-2}	T_M, K	T_{ES}, K
1.2×10^{17}	148,454	151.50
8×10^{16}	201,906	194.94
5×10^{16}	262,951	320.4
2×10^{16}	69,232	113.89

Table 2. Mott characteristic temperature and Efros-Shklovskii characteristic temperature at each irradiation dose.

Table 2 indicates that T_M is much higher than T_{ES}, this table also clears the coexistence of Mott variable range hopping mechanisms of conduction, and Shklovskii and Efros percolation mechanism of conduction, the coexistence of both models explained the low temperature conduction mechanisms reported [31, 32] in different compositions. But it is not clear up to now, are these two mechanisms of conduction simultaneously exist or consecutively one mechanism dominates in a certain temperature range and then, the other one. **Figure 10** shows the dependence of σ_o on the irradiation dose ϕ, the experimentally obtained data are fitted with Eq. (17)

$$\ln \phi = \frac{\ln \sigma_o}{a + b\ln \sigma_o + c\sqrt{\ln \sigma_o}} \tag{18}$$

where a, b, and c are coefficients to fit present experimental data, a = 777.8, b = 18, and c = 238.4. **Figure 10** shows that the pre-exponential factor ρ decreases with increase the irradiation fluency until reaching to minimum value and start to increasing this behavior could be explained as follows, as the irradiation dose increases the charge carrier increases, which causes a diminution of the resistivity until the concentration of charge carrier reaches its critical

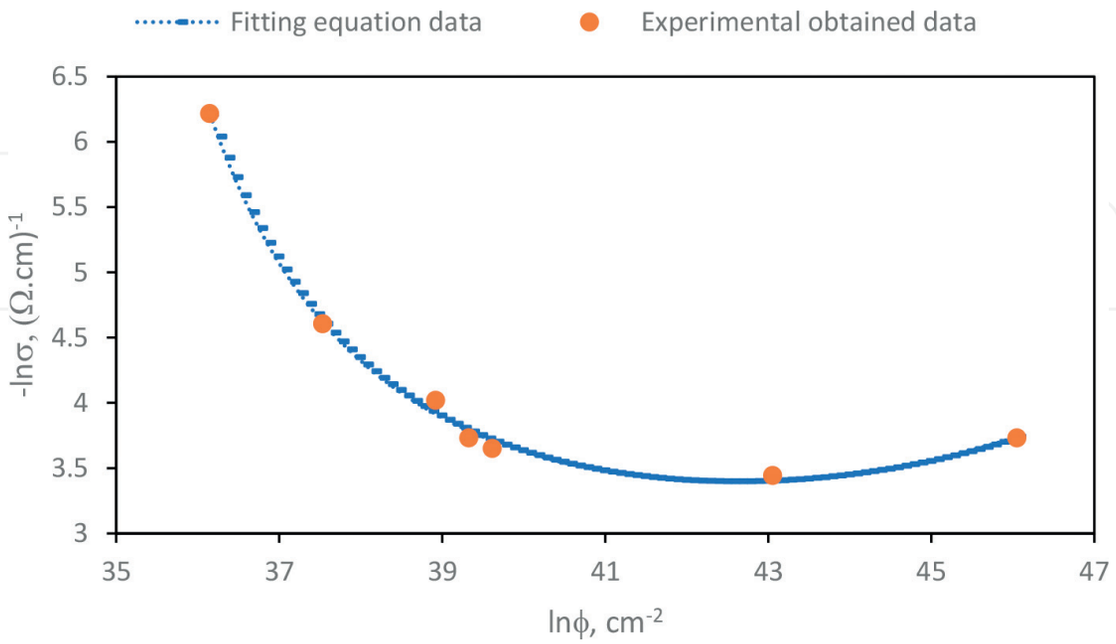

Figure 10. Fitting of Eq. (17) for the dependence of pre-exponential factor σ_o on the irradiation flux (φ).

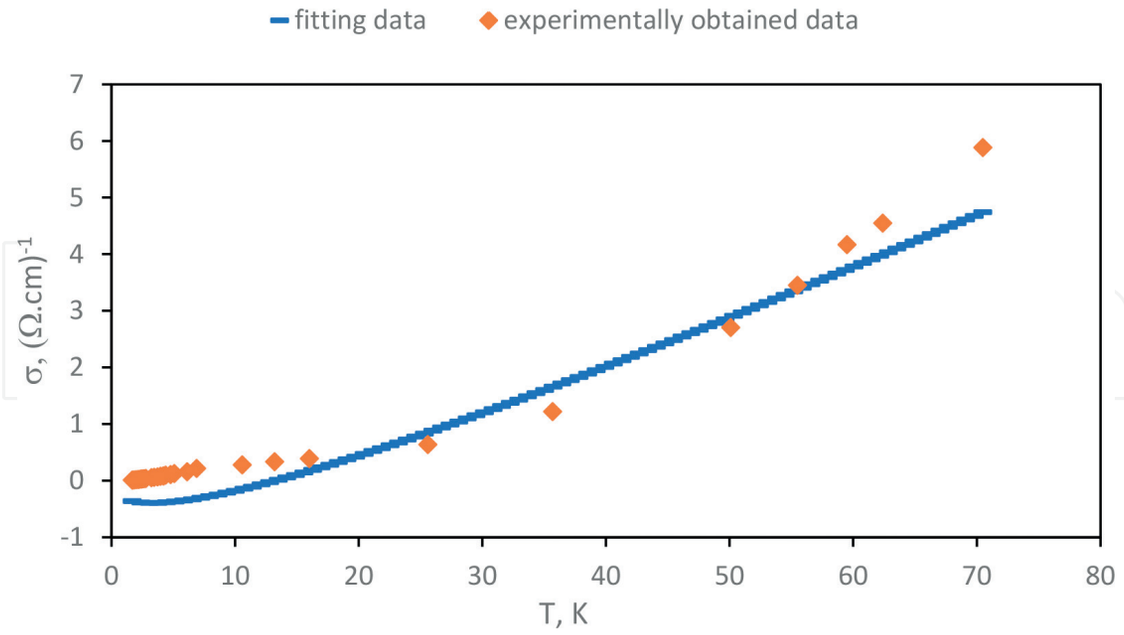

Figure 11. Fitting of Eq. (3) for dependence of conductivity on temperature of sample irradiated 5×10^{18} cm^{-2}.

value at which sample behaves as metallic like conductivity. In metallic conductors, the charge carrier augmentation enhances the possibility of collision between the charge carriers and with the doping centers, this increases the resistivity.

Figure 11 shows the fitting of conductivity dependence on temperature of sample irradiated with dose of 5×10^{18} cm^{-2} to equation [33]

$$\sigma = \sigma(0) + aT^{0.5} + bT \tag{19}$$

where $\sigma(0)$ is the residual conductivity at 0 K, the second and third term are related to weak localization effect. The fitting parameters as obtained from this equation are $\sigma(0) = 0$, a = −0.37, and b = 0.12.

Figure 12 shows the fitting of conductivity dependence on temperature of sample irradiated with irradiation dose 1×10^{20} cm^{-2} using Eq. (19). The fitting parameters as obtained from this equation are $\sigma(0) = 0$, a = 0.65, and b = 0.065.

Since we have insulator metal transition, this means that the sample starts as an insulator, but because of irradiation the same samples becomes a metallic-like conductor after certain irradiation dose. This means that the conduction in a material may behave like semiconductor (insulator) or metallic characteristic of conduction. The same equation, Eq. (19), did not fit the conductivity temperature dependence of sample irradiated with dose 1.6×10^{17} cm^{-2}. This means that this sample is in the insulator side of conductivity. However, the sample irradiated with dose 5×10^{18} is in the metallic conductivity side. For sample with irradiation dose 5×10^{18} cm^{-2}, the fitting parameter value is −0.037, the negative value of parameter a is reported in [34]. The negative value of a in some samples appears only at the beginning of metallic conductivity. From experimental data analysis of **Figure 7**, the extrapolation intercept with ordinate axes gives the resistivity, σ_o value. For sample irradiated with dose 1×10^{20} and

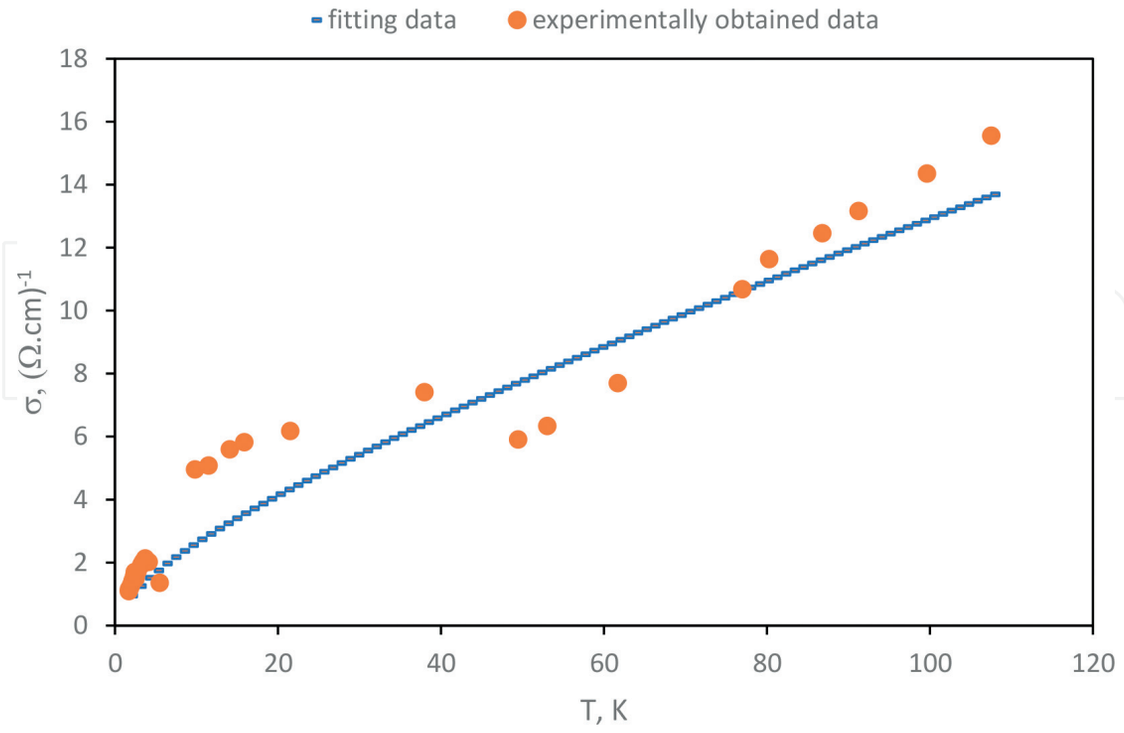

Figure 12. Fitting of dependence of conductivity on temperature of sample irradiated 1×10^{20} cm^{-2}.

1.6×10^{17} cm^{-2}; $\sigma_o = 0.024$ and $\sigma_o = 0.032$ $(\Omega\text{-cm})^{-1}$, from these values, one can say that σ_o in the metallic side of conductivity is dependent on irradiation dose. **Figure 10** shows the dependence of pre-exponential factor on neutron irradiation dose, it is clear that as the neutron irradiation dose increases, the value of the pre-exponential factor decreases. It reaches its minimum value at neutron irradiation dose 1.6×10^{17} cm^{-2} and starts to increase. Mott predicted that the minimum metallic conductivity $\sigma_{min} = \frac{0.026e^2}{\hbar a}$. In case of a = 2 Å, he predicted minimum metallic conductivity to be of the range 2–5000 $(\Omega.cm)^{-1}$, and he considered that this is the smallest conductivities to be expected, unless the density of states broadened by disorder. In this work samples irradiated with neutron flux 1×10^{20} and 5×10^{18} cm^{-2}, having minimum metallic conductivity equals to 0.024 and 0.032 $(\Omega\text{-cm})^{-1}$, respectively, these values are much smaller than the minimum value of metallic conductivity predicted by Mott. This may be due to the high disorder in germanium caused by neutron irradiation, or the Mott minimum metallic conductivity satisfied in materials just began its metallic conductivity behavior.

Figure 13 shows the dependence of $\ln(\rho_3)$ on average impurity center distance as predicted by Mott variable range hopping model, the relation between ρ_3 on the average impurity center distance is

$$\rho_3 = \rho_{03} e^{\frac{\alpha}{N_A a}}, \ \alpha = 1.74 \tag{20}$$

where ρ is the resistivity, α is a constant, N_A is the concentration of acceptor impurity centers per cm^{-3}, and a is the Bohr localization radius. From the line slope of **Figure 13**, the Bohr radius of localization is calculated and found equal to 43 Å, which is very close to the value of Bohr radius of localization at insulator metal transition which is 40 Å.

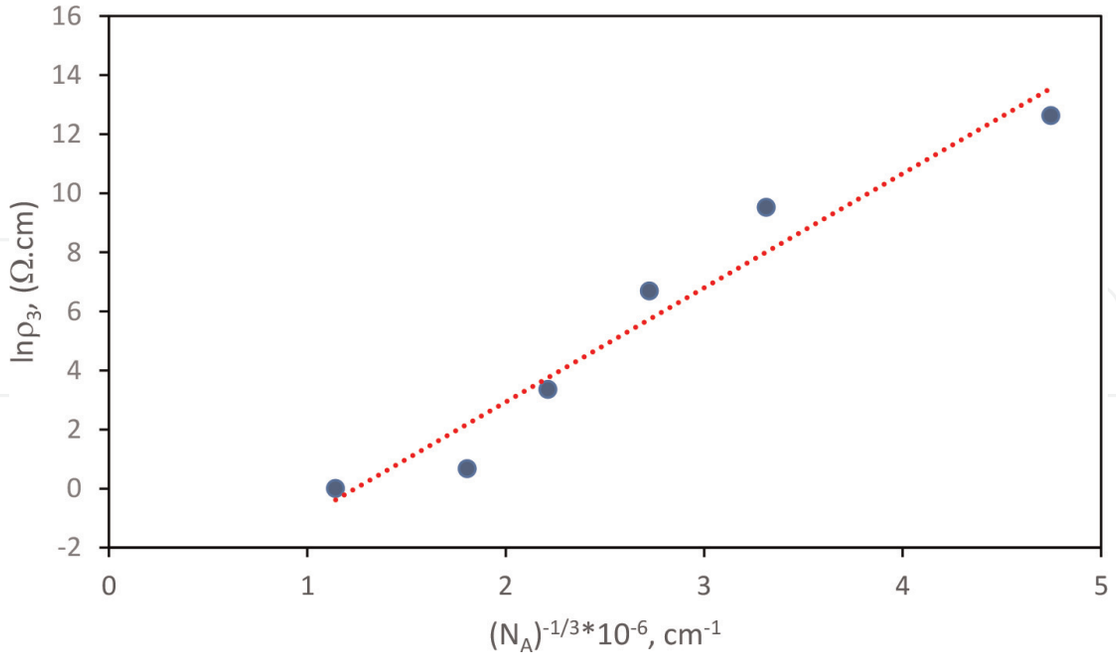

Figure 13. The dependence of ln $\rho_3$on average impurity center distance $(N_A)^{1/3}$.

6. Conclusions

The overall obtained results reveal that the n-type germanium is converted into p-type germanium by a fast reactor neutron irradiation. From analysis of the dependence, the electrical conductivity on temperature, the activation energies of conduction at different conductivity mechanism that; $E_1 > E_2 > E_3$ and the pre-exponential factors $\rho_2 > \rho_1 > \rho_0$ were observed for each irradiation dose. But these values decrease with increasing irradiation dose. The metallic-like behavior starts at irradiation dose 5×10^{18} cm^{-2}. There are sweeping between Mott variable range hopping model and Efros-Shklovskii percolation model. Each model dominates in certain range of temperature. From analysis of Mott, variable range hopping the Bohr radius of localization at Insulator metal transition is obtained to be equal to 43 Å, and the obtained minimum metallic conductivity value is 0.024 $(\Omega\text{-cm})^{-1}$, which is much lower than the value predicted by Mott theory of insulator-metal transition.

Author details

Samy Abd-elhakim Elsayed

Address all correspondence to: samy.abdelhameed@science.bsu.edu.eg

New Materials and Renewable Energy Laboratory, Physics Department, Faculty of Science, Beni-Suef University, Beni-Suef, Egypt

References

[1] Hecht E. Optics. San Francisco, Boston, New York: Adison Wesley; 2002

[2] Das A, Ferbal T. Nuclear and Particle Physics. Toh Tuck Link, Singapore: World Scientific Publishing; 2003

[3] Haas EW, Martin JA. Nuclear transmutation doping from the view point of radioactivity formation. In: Messe JM, editor. Neutron Transmutation Doping in Semiconductors. New York and London: Plenum Press; 1979

[4] Heller EE. Isotopically Controlled Semiconductors. 2004. http://escholarship.org/uc/item/1621k38s

[5] Zabrodskii AG, Alekseenko MV. Fermi level scan spectroscopy of gap states in Ge and Si–Ge alloysbased on the kinetics of neutron transmutation doping. Physica B. 2006;**376-377**:253

[6] Edwards PP, Johnston RL, Rao CNR, Tunstall DP, Hensel F. The metal-insulator transition: A perspective. Philosophical Transactions of the Royal Society of London A. 1998;**356**

[7] Mott NF. Metal Insulator Transition. 2nd ed. London: Taylor & Francis; 1990, and references therein

[8] Duan F, Guojin J. Introduction to Condensed Matter Physics. Vol. VI. Toh Tuck Link, Singapore: World Scientific Publishing Company; 2005

[9] Mott NF. The electrical conductivity of transition metals. Proceedings of the Royal Society of London A. 1936;**153**:699

[10] Gutzwiller MC. Effect of correlation on the ferromagnetism of transition metals. Physics Review. 1964;**134**:4A

[11] Brinkman WF, Rice TM. Application of gutzwiller's variational method to the metal-insulator transition. Physical Review B. 1970;**2**:10

[12] Craig PP, Goldburg WJ, Kitchens TA, Budnick JI. Transport properties at critical points: The resistivity of s. Physical Review Letters. 1967;**19**:23, and references therein

[13] Fisher ME, Langer JS. Resistive anomalies at magnetic critical points. Physics Review. 1968;**20**:13

[14] deGennes PE, Friedel J. Anomalies de résistivité dans certains métaux magníques. Journal of Physics and Chemistry of Solids. 1958;**4**

[15] Heing KH, Monecke J. Conductivity of the four-point Hubbard Model. Physica Status Solidi. 1972;**49**:K139

[16] Hubbard J. Theory the connexion with many-body perturbation electron correlations in narrow energy bands. VI. Proceedings of the Royal Society of London A. 1967;**296**:100

[17] Mott NF, Kaveh M. Metal Insulator transitions in non-crystalline systems. Advances in Physics. 1985;**34**:3

[18] Ramirez R, Fallicov LM, Kimball J. Metal-insulator transitions: A simple theoretical model. Physical Review B. 1970;**2**:8

[19] Anderson PW. Absence of diffusion in certain random lattices. Physics Review. 1958;**109**: 1492

[20] Crawford JH Jr, Cleland JW. Nature of bombardment damage and energy levels in semiconductors. Journal of Applied Physics. 1959;**30**(6):1204

[21] Crawford JH Jr, Lark-Horovitz K. Fast neutron bombardment effects in germanium. Physics Review. 1950;**78**:815

[22] Cleland JW, Crawford JH, Pigg JC. Transmutation-produced germanium semiconductors. Physics Review. 1950;**78**:814

[23] James HM, Lark-Horovitz K. Localized electronic states in bombarded semiconductors. Zeitschrift für Physikalische Chemie. 1951;**198**:107

[24] Fritzche H, Lark Horovitz K. The electrical properties of germanium semiconductors at low temperature. Physica A. 1954:834-844

[25] Dobrego VP, Ermolaev OP, Tkachev VD. Investigation of shallow radiation defect levels produced in Ge by fast neutron irradiation. Physica Status Solidi. 1977;**44**:435

[26] Konopleva RF, Novikov SR. Measuring the relative fast-neutron flux distribution in the VVR-M reactor with semiconductor detecting elements. Atomnaya Energiya. 1961;**11**:545. in Russian

[27] Fritzche H. Resistivity and hall coefficient of antimony doped germanium at low temperature. Journal of Physics and Chemistry of Solids. 1958;**6**:69

[28] Mott NF, Davis EA. Electronic Processes in Non-Crystalline Materials. Oxford: Clarendon Press; 2012

[29] Shklovskii BI, Efros AL. Electronic Properties of doped Semiconductors. Berlin, Heidelberg, New York, Tokyo: Springer-Verlag; 1984

[30] Elhakim SA, Morsy MA. Simultaneous $\gamma(Co^{60})$-quanta irradiation and isothermal annealing-induced insulator–metal transition in a-$As_4Se_4Te_2$ chalcogenide composition. Radiation Effects and Defects in Solids. 2014;**169**:4

[31] El-Sayed A. Fractal explanation of Meyer-Neldel rule. Journal of Non-Crystalline Solids. 2017;**458**:137-114

[32] El-hakim SA. Observation compensation effect and crossover between Percolation and variable-range-hopping regimes for dc conductivity in germanium irradiated with large fluencies fast neutrons. Journal of Optoelectronics and Advanced Materials. 2014;**16**(11–12): 1367

[33] Kawade K, Suzuki A, Tanka K. Electronic structure and electrical conductivity of amorphous Si–Ti alloys manifesting the metal-insulator transition. Journal of the Physical Society of Japan. 2000;**69**(3):777

[34] Hussey NE, Tanaka K, Takagi H. Universality of the Mott–Ioffe–Regel limit in metals. Philosophical Magazine. 2004;**84**(24):2847

IntechOpen

IntechOpen